Liquid Crystals
Publication details, including instructions for authors and subscription information:
http://www.informaworld.com/smpp/title~content=t713926090

Monofluorinated unsymmetrical bent-core mesogens

Remko Achten[a]; Evelien A. W. Smits[a]; R. Amaranatha Reddy[b]; Marcel Giesbers[a]; Antonius T. M. Marcelis[a]; Ernst J. R. Sudhölter[a]
[a] Laboratory of Organic Chemistry, Wageningen University, 6703 HB Wageningen, The Netherlands [b] Institute of Organic Chemistry, Martin-Luther-University Halle-Wittenberg, 06120 Halle (Saale), Germany

To cite this Article Achten, Remko , Smits, Evelien A. W. , Reddy, R. Amaranatha , Giesbers, Marcel , Marcelis, Antonius T. M. and Sudhölter, Ernst J. R.(2006) 'Monofluorinated unsymmetrical bent-core mesogens', Liquid Crystals, 33: 1, 57 — 65
To link to this Article: DOI: 10.1080/02678290500393131
URL: http://dx.doi.org/10.1080/02678290500393131

Liquid Crystals, Vol. 33, No. 1, January 2006, 57–65

Monofluorinated unsymmetrical bent-core mesogens

REMKO ACHTEN†, EVELIEN A. W. SMITS†, R. AMARANATHA REDDY‡, MARCEL GIESBERS†, ANTONIUS T. M. MARCELIS*† and ERNST J. R. SUDHÖLTER†

†Laboratory of Organic Chemistry, Wageningen University, Dreijenplein 8, 6703 HB Wageningen, The Netherlands
‡Institute of Organic Chemistry, Martin-Luther-University Halle-Wittenberg, Kurt-Mothes-Str.2, 06120 Halle (Saale), Germany

(*Received 16 May 2005; in final form 7 September 2005; accepted 10 September 2005*)

The synthesis and mesomorphic properties of 30 bent-core compounds with a fluorine substituent in one of the outer rings are reported. The banana-shaped compounds are all derived from resorcinol and contain esters as linking groups between the five aromatic rings. The different mesophases have been characterized by polarizing optical microscopy, differential scanning calorimetry, X-ray diffraction studies and electro-optical investigations. The compounds with the longer terminal chains exhibit an antiferroelectric SmCP phase. Upon introduction of a fluorine substituent the layer spacing increases, as compared with the corresponding unsubstituted compound. The introduction of one terminal vinyl group in the mono-substituted bent-core mesogens has no significant influence on the liquid crystalline properties and the switching remains antiferroelectric. Due to the introduction of the terminal double bond, these banana-shaped compounds are suitable for the preparation of siloxane polymers or attachment to a hydrogen-terminated silicon surface.

1. Introduction

Before 1996 all (anti)ferroelectric smectics were composed of tilted enantiomerically enriched molecules. In 1996 however, Niori *et al*. [1] reported ferroelectricity in achiral banana-shaped molecules possessing C_{2v} symmetry. Since then a number of different, so-called B-phases have been discovered [2]. The most frequently described B-phase is the B_2 phase (SmCP), which in most cases is found for bent molecules with relatively long terminal tails [3]. Due to the synclinic and anticlinic layer organization of the molecules in a ferroelectric or antiferroelectric polar order, four types of layer organization in the SmCP phase are possible [4]. As a result of the close packing of these bent-core mesogens there is limited rotational freedom around their molecular long axis. Recently it was shown, however, that some compounds do show collective rotation around the molecular long axis under an external electric field with some special experimental conditions, which can result in field-induced switching of supramolecular chirality [5, 6].

Among the more than a thousand banana-shaped molecules reported to date [2, 3, 7] several structural variations have been introduced to study their influence on the liquid crystalline properties. The influence of lateral substituents [8–13] and especially of fluoro-substituents, has been studied extensively. The polar fluorine substituents can be introduced symmetrically at both arms of the molecules [8–12, 14–21], but also non-symmetrically at only one arm of the molecule [22–24] or at the core, *e.g.* at a 3,4′-biphenyl central unit [25].

In this paper we study the influence of mono-fluoro substitution in one of the outer phenyl rings, *ortho* to the terminal tail of an ester-connected bent-core mesogen, series *m*-**P**-F*n* (scheme 1). Part of this series has already been studied by Shreenivasa Murthy *et al*. [23]. It is known that the antiferroelectric ground state of compounds without substituents, can change to ferroelectric upon introduction of F-substituents at this special position in both arms of the molecule [15, 19, 21, 26]. Additionally, we have synthesized a second series in which one terminal double bond is introduced into the mono-fluorinated mesogen, series 11a-**P**-F*n* (scheme 1).

2. Experimental

2.1. *Synthesis*

The compounds of series *m*-**P**-F*n* were prepared according to scheme 2. The monosubstituted resorcinol derivatives **P**-*m* were synthesized according to a literature procedure [27]. 4-Bromo-2-fluorophenol was obtained from Aldrich and used without further purification. The compounds from series 11a-**P**-F*n* were

*Corresponding author. Email: ton.marcelis@wur.nl

Liquid Crystals
ISSN 0267-8292 print/ISSN 1366-5855 online © 2006 Taylor & Francis
http://www.tandf.co.uk/journals
DOI: 10.1080/02678290500393131

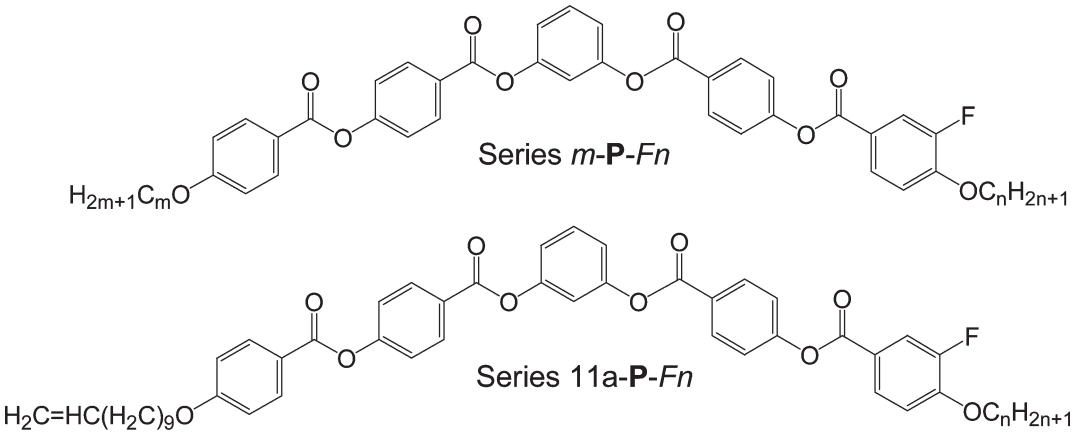

Scheme 1. Bent-core structures of the compounds of series *m*-**P**-F*n* and 11a-**P**-F*n*.

prepared according to the same procedure, by using **P**-11a [27] instead of **P**-*m*.

Compounds **I**-*n*F were obtained by etherification of 4-bromo-2-fluorophenol with the corresponding bromoalkanes (n=8, 10, 12, 14 and 16) and K_2CO_3 as base. **II**-*n*F was obtained by carboxylation of the Li-analogue of **I**-*n*F with carbon dioxide. Compounds **IV**-*n*F were obtained by esterification of the acid chlorides of **II**-*n*F with 4-hydroxybenzaldehyde (compound **III**-*n*F) followed by $NaClO_2$ oxidation [28]. The banana-shaped products (*m*-**P**-F*n*) were obtained by esterification of the acid chloride of **IV**-*n*F and **P**-*m* in THF with DMAP as base.

2.1.1. 4-Bromo-2-fluoro-1-tetradecyloxybenzene (I-14F). A mixture of 9.50 g (49.7 mmol) 4-bromo-2-fluorophenol, 15.13 g (54.6 mmol) 1-bromo-tetradecane and 11.2 g K_2CO_3 in 100 ml of butanone was heated under reflux overnight. After cooling, the mixture was concentrated and 100 ml CH_2Cl_2 added. After filtration of the salts the filtrate was concentrated and the colourless oil used in the next step without further purification; yield 95%. ^{1}H NMR (200 MHz, $CDCl_3$) δ (ppm): 7.18 (m, 2H, Ar), 6.81 (t, 1H, Ar), 3.98 (t, 2H, OCH_2), 1.83 (m, 2H, $OCCH_2$), 1.55–1.25 (m, 22H, $11\times CH_2$), 0.87 (t, 3H, CH_3). HRMS: calc. for $C_{20}H_{32}BrFO$ 386.1621; found 386.1617.

2.1.2. 3-Fluoro-4-tetradecyloxybenzoic acid (II-14F). To a solution of 18.37 g 4-bromo-2-fluoro-1-tetradecyloxybenzene (**I**-14F; 47.4 mmol) in 100 ml of dry THF at -60°C, was added 35.6 ml of a 1.6 M solution of butyllithium in hexane (57.0 mmol). After stirring for 0.5 h at -78°C, the cold solution was poured onto crushed solid CO_2, and allowed to warm to room temperature. Thereafter, the reaction mixture was acidified to pH 2 with a 10% HCl solution. Subsequently, the mixture was partially concentrated and the precipitate filtered off, and washed with water. Recrystallization from EtOH and washing with PE 40–60 gave white/yellow crystals; yield 14%, Cr 112 (N 109 I) ($^\circ$C). ^{1}H NMR (200 MHz, $CDCl_3$) δ (ppm): 7.82 (m, 2H, Ar), 6.98 (t, 1H, Ar), 4.09 (t, 2H, OCH_2), 1.85 (m, 2H, $OCCH_2$), 1.45–1.25 (m, 22H, $11\times CH_2$), 0.87 (t, 3H, CH_3). HRMS: calc. for $C_{21}H_{33}FO_3$ 352.2414; found 352.2417.

2.1.3. 4-(3-Fluoro-4-n-tetradecyloxybenzoyloxy)benzaldehyde (III-14F). Compound **II**-14F (2.28 g, 6.5 mmol) was heated under reflux in thionyl chloride (20 ml) for 2 h. Excess thionyl chloride was removed by distillation under reduced pressure. The resulting acid chloride was dissolved in 20 ml dry THF, and 0.79 g (6.5 mmol) 4-hydroxybenzaldehyde was added. To this clear solution 2 equivalents (1.58 g, 12.9 mmol) of DMAP were added, and the reaction mixture was stirred for 24 h at room temperature under a N_2 atmosphere. After removal of the THF, 200 ml of CH_2Cl_2 was added. The organic layer was washed with a 1M HCl solution ($2\times$) and a saturated $NaHCO_3$ solution and dried over Na_2SO_4. Multiple recrystallizations from EtOH yielded white crystals; yield 63%, Cr 86 (SmC 71 I) ($^\circ$C). ^{1}H NMR (400 MHz, $CDCl_3$) δ (ppm): 10.05 (s, 1H, CHO),7.99 (d, 3H, Ar), 7.92 (d, 1H, Ar), 7.43 (d, 2H, Ar), 7.07 (t, 1H, Ar), 4.15 (t, 2H, OCH_2), 1.90 (m, 2H, $OCCH_2$), 1.55–1.29 (m, 22H, $11\times CH_2$), 0.90 (t, 3H, CH_3). HRMS: calc. for $C_{28}H_{37}FO_4$ 456.2676; found 456.2680.

2.1.4. 4-(3-Fluoro-4-n-tetradecyloxybenzoyloxy)benzoic acid (IV-14F). Compound **III**-14F (1.85 g, 4.1 mmol) and resorcinol (0.58 g, 5.3 mmol) were dissolved in THF (50 ml). To this solution was added dropwise, over 10 min, a solution of sodium chlorite ($NaClO_2$, 80%; Aldrich) (2.13 g, 23.6 mmol) and sodium dihydrogenphosphate

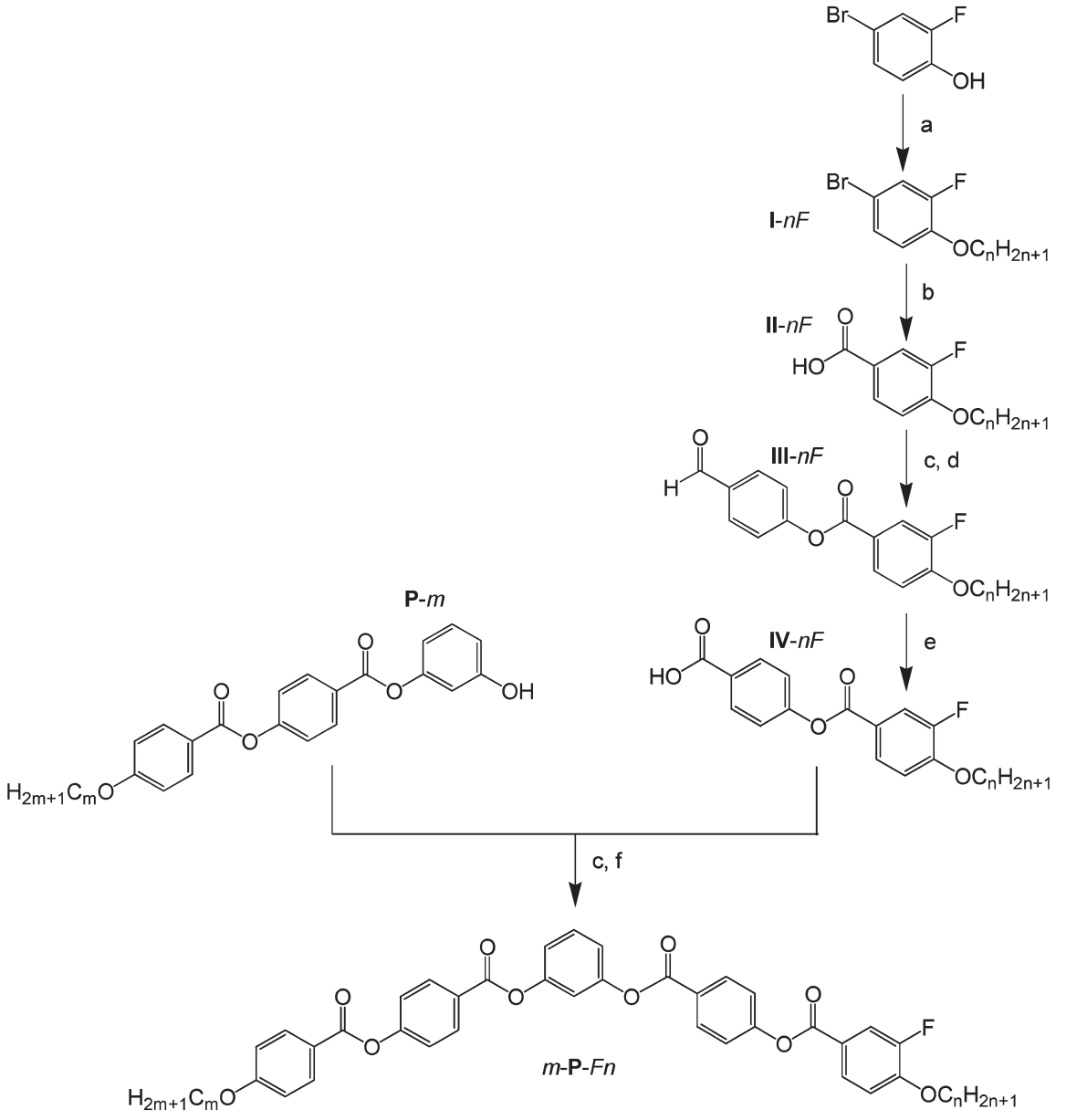

Scheme 2. Synthesis of compounds in series *m*-**P**-F*n*: (a) $H(CH_2)_nBr$ (n=8, 10, 12, 14, 16), K_2CO_3, butanone, reflux; (b) *n*-BuLi, −78°C, CO_2 (s); (c) $SOCl_2$, reflux; (d) 4-hydroxybenzaldehyde, DMAP, THF, rt; (e) $NaClO_2$, resorcinol, NaH_2PO_4, THF, H_2O, rt; (f) DMAP, THF, rt.

monohydrate (1.70 g, 12.3 mmol) in 20 ml water. The resulting pale yellow reaction mixture was then stirred overnight at room temperature. Volatile components were removed *in vacuo* and the residue dissolved in 100 ml water. The aqueous solution was acidified to pH 2 by adding 1M HCl. The white precipitate was filtered, washed with water, and dried in air. The white crystals were then washed with PE 40–60; yield 95%, Cr 140 SmC 190 N 207 I (°C). ^{1}H NMR (400 MHz, $CDCl_3$) δ (ppm): 8.19 (d, 2H, Ar), 7.99 (d, 1H, Ar), 7.95 (d, 1H, Ar), 7.34 (d, 2H, Ar), 7.07 (t, 1H, Ar), 4.15 (t, 2H, OCH_2), 1.89 (m, 2H, $OCCH_2$), 1.67–1.29 (m, 22H, $11 \times CH_2$), 0.91 (t, 3H, CH_3). HRMS: calc. for $C_{28}H_{37}FO_5$ 472.2625; found 472.2628.

2.1.5. 1-[4-(4-Decyloxybenzoyloxy)benzoyloxy]-3-[4-(3-fluoro-4-n-tetradecyloxybenzoyloxy)-benzoyloxy]benzene (10-P-F14). Compound **IV**-14F (0.15 g, 0.32 mmol) was refluxed in thionyl chloride (5 ml) for 2 h. Excess thionyl chloride was then removed by distillation under reduced pressure. The resulting acid chloride was dissolved in 8 ml freshly distilled dry THF and to this

stirred solution 0.16 g (0.32 mmol) of **P**-10 was added; 2 equiv of DMAP (0.08 g, 0.64 mmol) were then added. The reaction mixture was stirred for 24 h at room temperature under N_2. The THF was removed under *vacuo* and ~50 ml CH_2Cl_2 was added. The organic layer was washed successively with 1M HCl (2×) and a saturated $NaHCO_3$ solution, then dried over anhydrous Na_2SO_4. After filtration of the salts the filtrate was concentrated and the residue purified by column chromatography (eluant: 10% PE 40–60 in CH_2Cl_2). Finally, recrystallization from acetonitrile and washing with PE 40–60 gave colourless crystals; yield 53%. ^{1}H NMR (400 MHz, $CDCl_3$) δ (ppm): 8.31 (d, 4H, Ar), 8.18 (d, 2H, Ar), 8,00 (d, 1H, Ar), 7.93 (d, 1H, Ar) 7.53 (t, 1H, Ar), 7.40 (d, 4H, Ar), 7.22 (s+d, 3H, Ar), 7.07 (t, 1H, Ar), 7.02 (d, 2H, Ar), 4.16 (t, 2H, OCH_2), 4.08 (t, 2H, OCH_2), 1.88 (m, 4H, 2×$OCCH_2$), 1.57–1.29 (m, 36H, 18×CH_2), 0.91 (t, 6H, CH_3). ^{13}C NMR ($CDCl_3$) δ (ppm): 164.7, 164.5, 164.4, 164.2, 155.9, 155.6, 151.8, 132.8, 132.3, 130.5, 130.3, 128.0, 127.9, 127.2, 127.0, 122.6, 122.4, 121.3, 119.7, 118.4, 118.1, 116.2, 114.8, 113.8, 69.9, 68.8, 32.3, 30.1, 30.0, 29.9, 29.8, 29.7, 29.5, 29.4, 26.4, 26.3, 23.1, 14.5.

2.1.6. 1-{4-[4-(10-Undecenyloxy)benzoyloxy]benzoyloxy}-3-[4-(3-fluoro-4-n-tetradecyloxybenzoyloxy)benzoyloxy] benzene (11a-P-F14). This compound was prepared using the same procedure as for compound 10-**P**-F14 starting from **IV**-14F and **P**-11a; yield 73%. ^{1}H NMR (400 MHz, $CDCl_3$) δ (ppm): 8.21 (d, 4H, Ar), 8.08 (d, 2H, Ar), 7.90 (d, 1H, Ar), 7.83 (d, 1H, Ar) 7.42 (t, 1H, Ar), 7.30 (d, 4H, Ar), 7.11 (s+d, 3H, Ar), 6.97 (t, 1H, Ar), 6.91 (d, 2H, Ar), 5.73 (m, 1H, =CH), 4.88 (m, 2H, $=CH_2$), 4.05 (t, 2H, OCH_2), 3.97 (t, 2H, OCH_2), 1.97 (m, 2H, C=CCH_2), 1.77 (m, 4H, 2×$OCCH_2$), 1.65–1.11 (m, 34H, 17×CH_2), 0.81 (t, 3H, CH_3). ^{13}C NMR ($CDCl_3$) δ (ppm): 164.7, 164.5, 164.4, 164.2, 155.9, 155.6, 151.8, 139.6, 132.8, 132.3, 130.3, 128.0, 127.2, 127.0, 122.6, 122.5, 121.3, 119.7, 116.2, 114.8, 114.6, 113.8, 69.9, 68.8, 34.2, 32.3, 30.1, 30.0, 29.9, 29.8, 29.7, 29.5, 29.3, 26.4, 26.3, 23.1, 14.6.

2.2. *Measurements*

Melting points, thermal phase transition temperatures and optical inspection of the liquid crystalline phases were performed on samples between ordinary glass slides using an Olympus BH-2 polarizing microscope equipped with a Mettler FP82HT hot stage, which was controlled by a Mettler FP80HT central processor. Differential scanning calorimetry (DSC) thermograms were obtained on a Perkin Elmer DSC-7 system using 0.5–3 mg samples in 50 µl sample pans and a scan rate of 5°C min^{-1}. ΔH was determined in the third heating scan and calculated in kJ mol^{-1}. Temperature dependent X-ray curves were obtained on a Philips X'pert Pro MRD machine equipped with an Anton Paar camera for temperature control. For measurements in the small angle region the sample was spread in the isotropic or liquid crystalline phase on a thin glass slide (about 15 µm thick) which was placed on a temperature-regulated flat copper sample stage. The switching behaviour was determined using the triangular wave method with a 6 µm polyimide coated ITO cell and the cells were filled in the isotropic state. Electro-optical measurements were carried out using a combination of function synthesizer (Keithly, model 3910), amplifier (Krohn-Hite, model 7500), and the current response traces were recorded using an oscilloscope (Hewlett Packard, model 54610A) across a 5 kΩ resistance.

3. Results and discussion

3.1. *The m-P-Fn series*

The transition temperatures and associated enthalpy changes of the compounds in the *m*-**P**-F*n* series are given in table 1. Five of the 25 compounds studied in this series have already been described and characterized by Shreenivasa Murthy and Sadashiva [23] and we obtained similar transition temperatures. Compound 8-**P**-F8 is the only one in this series that has a monotropic columnar B_1 phase. All other compounds in the *m*-**P**-F*n* series show enantiotropic liquid crystalline SmCP phases. The melting points and isotropization temperatures are also presented in 3D graphs (figures 1 and 2). Figure 1 shows that all compounds with $m=n$ exhibit a maximum in melting point. In series *m*-**P**-F12, for example, the analogue with $m=12$ has the highest melting point. Remarkably, symmetric compounds exhibit higher melting points than their non-symmetric analogues [29]. This is a clear indication that the unsymmetrical compounds show reduced packing efficiency and hence lower melting points. In this case however, none of the molecules in the *m*-**P**-F*n* series is truly symmetric due to the fluorine atom in only one of the arms. The influence of one small polar substituent on the melting point is apparently very small. The transition temperatures, of homologues with equal $m+n$, are barely influenced by the presence of the F-atom in either the ring connected to the shortest (*e.g.* 16-**P**-F14) or the longest (*e.g.* 14-**P**-F16) terminal tail.

In most cases the isotropization temperatures gradually increase and reach a plateau value upon increasing *m* or *n* (figure 2), as observed in several other series of banana-shaped compounds [19]. On cooling from the isotropic phase the SmCP compounds all show a grainy unspecific texture under polarizing optical microscopy.

Table 1. Transition temperatures (°C), transition enthalpies (kJ mol^{-1}; between square brackets) and layer spacings d (Å) of the compounds in series *m*-**P**-F*n*.

Compound	Cr	B_1	$SmCP_A$	I	d
8-**P**-F8	• 121 [36.4]	(• 114) [11.3 [a]]		•	—
10-**P**-F8	• 100 [16.8]		• 113 [19.3]	•	34.4
12-**P**-F8 [23]	• 100 [17.2]		• 114 [19.6]	•	36.0
14-**P**-F8	• 95 [12.3]		• 115 [19.5]	•	38.1
16-**P**-F8	• 95 [13.7]		• 114 [19.7]	•	39.6
8-**P**-F10	• 108 [22.4 [a]]		• 113 [18.3 [a]]	•	34.7
10-**P**-F10	• 112 [20.9]		• 119 [19.2]	•	36.0
12-**P**-F10 [23]	• 102 [20.3]		• 119 [21.2]	•	37.6
14-**P**-F10	• 99 [19.1]		• 120 [21.6]	•	38.6
16-**P**-F10	• 95 [14.1]		• 120 [20.5]	•	40.0
8-**P**-F12	• 101 [18.0]		• 114 [19.4]	•	36.0
10-**P**-F12	• 105 [28.2]		• 119 [19.7]	•	37.2
12-**P**-F12 [23]	• 108 [23.3]		• 124 [21.8]	•	38.3
14-**P**-F12	• 101 [22.6]		• 123 [22.9]	•	39.5
16-**P**-F12	• 95 [21.5]		• 122 [23.1]	•	40.7
8-**P**-F14	• 101 [19.1]		• 116 [20.4]	•	37.4
10-**P**-F14	• 99 [20.3]		• 120 [21.9]	•	38.4
12-**P**-F14 [23]	• 102 [23.1]		• 122 [23.1]	•	39.7
14-**P**-F14	• 104 [25.8]		• 124 [23.6]	•	40.5
16-**P**-F14	• 99 [25.6]		• 124 [24.5]	•	42.0
8-**P**-F16	• 98 [18.6]		• 115 [16.6]	•	38.9
10-**P**-F16	• 98 [19.0]		• 121 [19.6]	•	40.1
12-**P**-F16 [23]	• 97 [22.6]		• 123 [23.2]	•	41.0
14-**P**-F16	• 95 [31.0]		• 122 [23.8]	•	42.3
16-**P**-F16	• 102 [43.6]		• 124 [23.9]	•	43.1

[a]Determined upon cooling.

Sometimes domains of opposite handedness, but with the typical SmCP fringe pattern, were observed. As anticipated, the compounds all behave quite similarly; the SmCP mesophase range varies between 5 and 27°C. Only one compound, with the shortest terminal tails, 8-**P**-F8, showed a mosaic-like texture typical for the columnar B_1 (Col_r) phase. Due to partial crystallization we were unable to carry out X-ray diffraction (XRD) measurements for 8-**P**-F8 in the liquid crystalline phase. XRD experiments were carried out on the other 24 compounds in the *m*-**P**-F*n* series. For these SmCP compounds usually two reflections (1 0 0 and 2 0 0) in the small angle region were observed. The corresponding d-spacings are summarized in table 1 and figure 3. There is an almost linear relationship between the number of carbon atoms in one of the terminal tails

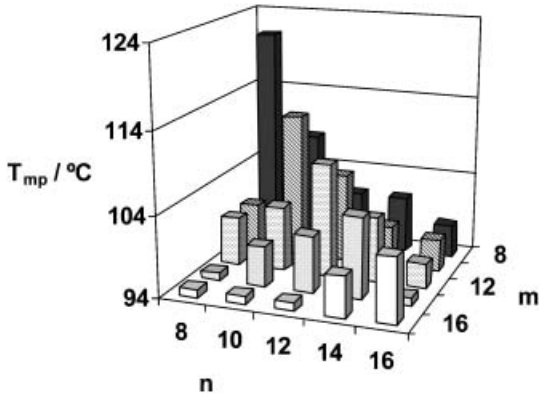

Figure 1. 3D representation of the melting points of the compounds from series *m*-**P**-F*n*.

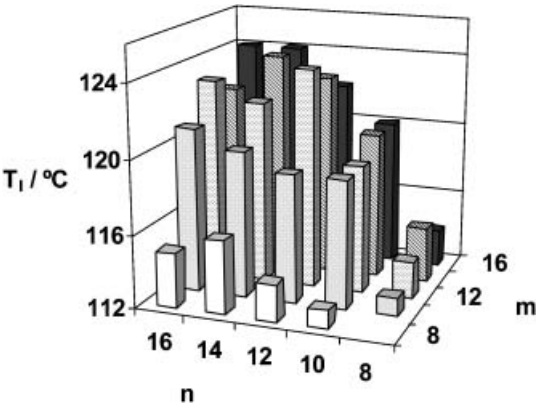

Figure 2. 3D representation of the isotropization temperatures (only SmCP–I transitions) of the compounds in series *m*-**P**-F*n*.

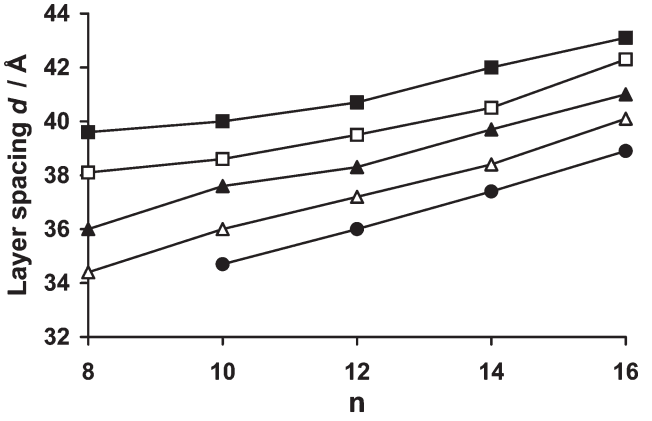

Figure 3. Dependence of the layer spacing *d*, on *m* and *n* of the compounds in series *m*-**P**-F*n* (*m*=8 ●; 10 △; 12 ▲; 14 □; 16 ■).

and the layer spacing *d*. As discussed [23], the SmCP compounds in the *m*-**P**-F*n* series show antiferroelectric switching properties upon application of a normal as well as a modified triangular-wave electric field.

3.2. *The m-P-Fn series in comparison with the m-P-n and mF-P-Fn series*

First, we compare the mono-fluorinated molecules with two terminal tails of the same length (*m*-**P**-F*n* series; *m*=*n*), with the corresponding compounds with no (*m*-**P**-*n* series; *m*=*n*) [19, 27] or two (*m*F-**P**-F*n* series; *m*=*n*) [19, 20] fluoro-substituents (figure 4).

Fluorine substitution *ortho* to the alkoxy chains stabilizes the liquid crystalline phase, since the isotropization temperatures increase upon introduction of F-substituents, figure 4. The isotropization temperatures of the compounds with one F-substituent are in between those with no or two F-substituents. The mesophase range, on the other hand, is largest for the series with one F-substituent. The mesophase range of series *m*-**P**-*n* is relatively small with a maximum of ~12°C [19, 27]. For the compounds with one F-substituent, a larger mesophase range is found (up to ~27°C). Surprisingly, the melting points of series *m*-**P**-F*n* and *m*-**P**-*n* (*m*=*n*) are rather similar, and significantly lower than for series *m*F-**P**-F*n* (*m*=*n*). Compound 10F-**P**-F10, and probably also 8F-**P**-F8, are not liquid crystalline due to their high melting points [19]. Therefore the *m*F-**P**-F*n* series shows the smallest mesophase range.

On going from series *m*-**P**-*n* and *m*-**P**-F*n* (*m*=*n*; with no or one F-substituent), to the difluoro-substituted compounds (*m*F-**P**-F*n* series; *m*=*n*) the switching behaviour changes from AF to FE [19, 23]. Compounds 12F-**P**-F12, 14F-**P**-F14 and 16F-**P**-F16 exhibit a ferroelectric switching SmCP phase, with synclinic tilt organization; SmC_SP_F [20]. In other series of bent-core mesogens it has also been shown that F-substitution at the *ortho* position to the terminal tails, can induce ferroelectric switching [26]. Apparently, both arms of the molecules need to be substituted by a fluorine atom to change the switching behaviour from AF to FE. In contrast to the other positions on the rings, disubstitution *ortho* to the alkoxy chains significantly increases the layer spacing *d* when compared with the non-substituted parent compounds [19]. The intermediate compounds with only one F-substituent all show intermediate layer spacing as shown in figure 5. However, at present the reason for this is not clear although may be explained in two possible ways. One explanation is that a F-substituent at this position induces a change (decrease) in tilt angle. When a second F-substituent is introduced the tilt angle decreases further resulting in a change of layer organization from AF to FE. This could however not be verified, since no X-ray patterns of oriented domains could be obtained. The second possibility could be that the fluorine substitution at the *ortho*

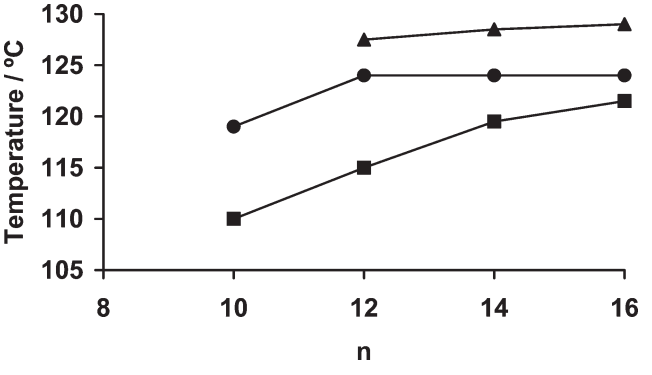

Figure 4. Comparison of the isotropization temperatures for the compounds of series *m*-**P**-*n* [19, 27] (■), *m*-**P**-F*n* (●) and *m*F-**P**-F*n* [19, 20] (▲) (*m*=*n*).

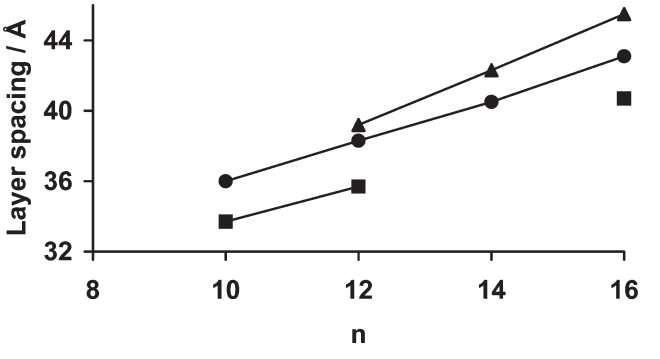

Figure 5. Comparison of layer spacings *d* for the compounds of series *m*-**P**-*n* [19, 27] (■), *m*-**P**-F*n* (●) and *m*F-**P**-F*n* [19, 20] (▲) (*m*=*n*).

position to the alkoxy chains can change the inter-layer interactions at the inter-layer interfaces. The ferroelectric organization, for example, decreases the inter-layer interactions, which obviously increases the layer spacing.

The non-F-substituted compounds (10-**P**-*n* series) with two terminal tails of different lengths described previously [29], are compared with the mono fluoro-substituted series 10-**P**-F*n* and *m*-**P**-F10. In all cases the isotropization temperatures of the F-substituted compounds are ~8°C higher than the corresponding non-fluorinated compounds. The layer spacings *d* are 2.3 to 3.0 Å larger for the analogous mono-fluoro compounds with the same tail lengths.

3.3. *The 11a-P-Fn series*

The thermotropic properties of the double bond terminated compounds in series 11a-**P**-F*n*, having in all 5 compounds one undecenyloxy chain with a terminal vinyl group, are summarized in table 2. All the compounds are liquid crystalline and exhibit the $SmCP_A$ phase, similar to the compounds from the *m*-**P**-F*n* series. The mesophase range increases with *n*. Surprisingly, the isotropization temperatures (and also the melting points) of the compounds in series 11a-**P**-F*n* show more similarities with series 11-**P**-*n* [29] than with 11a-**P**-*n* [29], as shown in figure 6. This can be explained by realizing that introducing a terminal vinyl group lowers the isotropization temperatures [29], and a F-substituent increases the isotropization temperature. Just as in series *m*-**P**-F*n*, the isotropization temperatures of compounds in series 11a-**P**-F*n* are higher (5 or 6°C) than the analogues with no fluorine substituents. In contrast to the short-tailed compounds ($n=8$) from series 11-**P**-*n* and 11a-**P**-*n*, which exhibit a B_1 phase, compound 11a-**P**-F8 shows the SmCP phase. Apparently the polar F-substituent stabilizes the SmCP phase. The XRD data, figure 7, show that the *d*-spacings for compounds 11a-**P**-F*n* are 2 or 3 Å larger than for the corresponding compounds without the F-substituent, 11a-**P**-*n*, and also for series 11-**P**-*n* [29].

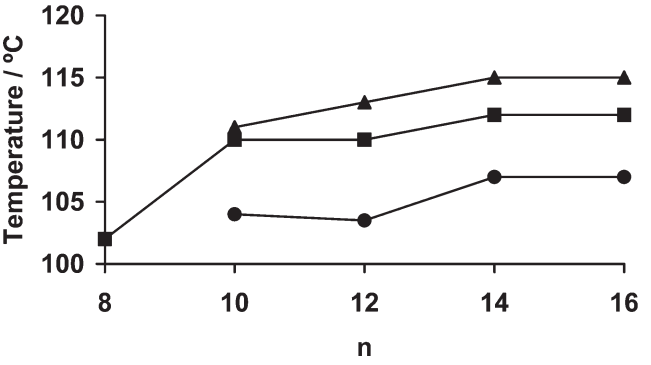

Figure 6. Comparison of the isotropization temperatures for the compounds of series 11-**P**-*n* [29] (▲), 11a-**P**-F*n* (■) and 11a-**P**-*n* [29] (●).

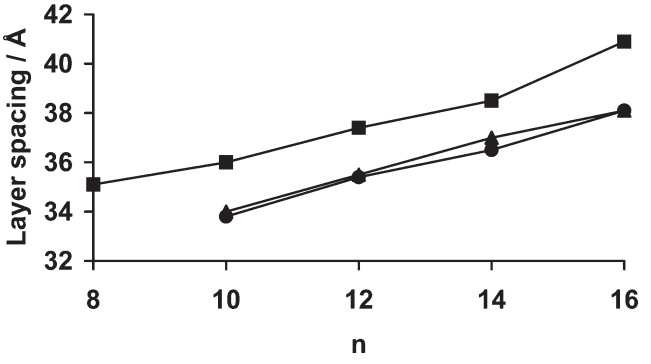

Figure 7. Comparison of layer spacings *d* for the compounds of series 11-**P**-*n* [29] (▲), 11a-**P**-F*n* (■) and 11a-**P**-*n* [29] (●).

The optical texture of the vinyl-terminated series shows a grainy texture; but also chiral domains of opposite handedness, as shown for compound 11a-**P**-F14 (figure 8), are observed upon slightly decrossing the polarizers. These observations show that an anticlinic antiferroelectric correlation in adjacent layers is present (SmC_AP_A). The electro-optical switching properties were investigated for a short (11a-**P**-F8) and a long (11a-**P**-F14) homologue in this series. Compound

Table 2. Transition temperatures (°C), transition enthalpies (kJ mol^{-1}; between square brackets) and layer spacings *d* (Å) of the compounds in series 11a-**P**-F*n*.

Compound	Cr	$SmCP_A$	I	*d*
11a-**P**-F8	• 97 [17.0 [a]]	• 102 [17.3 [a]]	•	35.1
11a-**P**-F10	• 101 [b]	• 110 [b]	•	36.0
11a-**P**-F12	• 98 [19.5]	• 110 [18.2]	•	37.4
11a-**P**-F14	• 93 [19.9]	• 112 [21.4]	•	38.5
11a-**P**-F16	• 90 [14.9]	• 112 [18.2]	•	40.9

[a]Determined upon cooling; [b]Could not be determined.

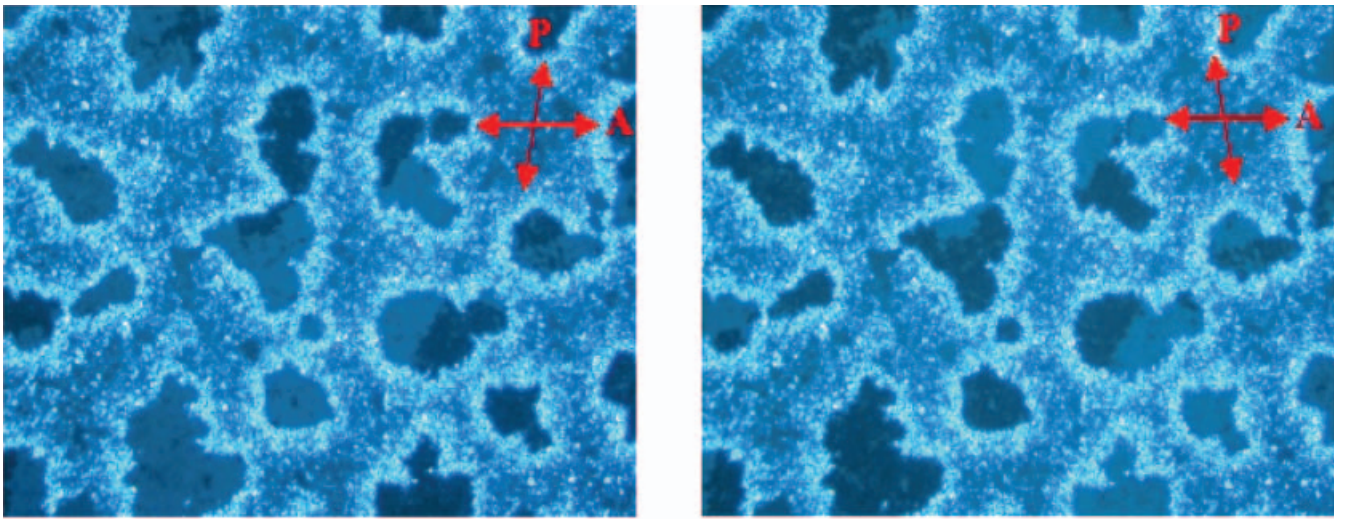

(*a*) (*b*)

Figure 8. Optical photomicrographs obtained for the mesophase of compound 11a-**P**-F14 as seen between slightly decrossed (5–10°) polarizers in either one (*a*) or the other (*b*) direction.

11a-**P**-F14 showed, on application of a triangular-wave voltage (threshold: 160 V_{pp} for a 6 µm cell at 10 Hz), two polarization current peaks for each half-period of the wave, figure 9. This indicates antiferroelectric tristable switching for the SmCP mesophase, with a spontaneous polarization of ~1100 nC cm^{-2} at 95°C. Under these experimental conditions, a more birefringent fan-shaped texture was obtained, stable for several hours even after removal of the applied field (surface alignment effect). The short-tailed homologue, 11a-**P**-F8, showed the same optical and switching properties ($\mathbf{P}_S$ ~950 nC cm^{-2} at 95°C).

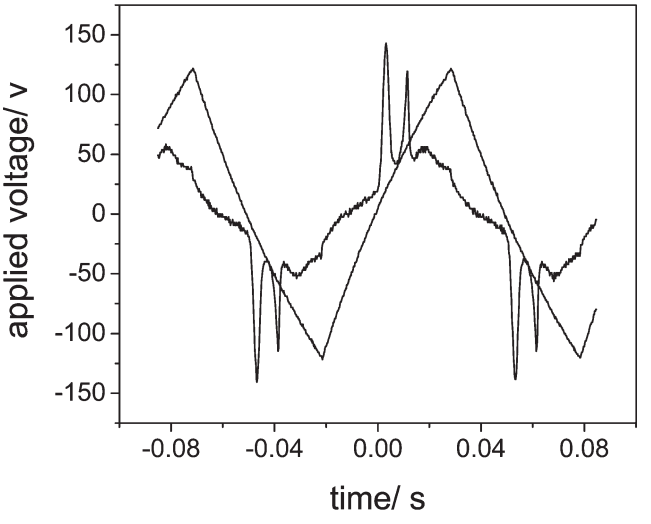

Figure 9. Switching current response trace obtained for compound 11a-**P**-F14 on applying a triangular-wave voltage (240 V_{pp} for 6 µm cell thickness, at 10 Hz).

4. Conclusions

The influence of a fluoro-substituent, at the *ortho* position with respect to the alkoxy group in one of the outer aromatic groups of a five-ring banana-shaped molecule has been studied. In contrast to the difluoro-substituted compounds, which show ferroelectric switching, these compounds exhibit a SmCP mesophase with antiferroelectric switching properties. The layer thickness of the compounds in the SmCP phase are intermediate between the non- and difluoro-substituted compounds. The SmCP phase is slightly stabilized upon introduction of one F-substituent, since compounds with relatively short terminal chains also show this mesophase. A second mono-fluorinated series, in which one of the terminal alkoxy chains is replaced by an undecenyloxy tail, exhibits similar SmCP phases. As in the previously described series, the ground state of the vinyl-terminated banana compounds is antiferroelectric. Due to the terminal vinyl groups these molecules are suitable for attachment to hydrogen-terminated silicon species via a hydrosilylation reaction.

References

[1] T. Niori, F. Sekine, J. Watanabe, T. Furukawa, H. Takezoe. *J. mater. Chem.*, **6**, 1231 (1996).
[2] G. Pelzl, S. Diele, W. Weissflog. *Adv. Mater.*, **11**, 707 (1999).
[3] D. Shen, A. Pegenau, S. Diele, I. Wirth, C. Tschierske. *J. Am. chem. Soc.*, **122**, 1593 (2000).

[4] D.R. Link, G. Natale, R. Shao, J.E. Maclennan, N.A. Clark, E. Körblova, D.M. Walba. *Science*, **278**, 1924 (1997).
[5] C. Keith, R. Amaranatha Reddy, U. Baumeister, C. Tschierske. *J. Am. chem. Soc.*, **126**, 14312 (2004).
[6] R. Amaranatha Reddy, M.W. Schröder, M. Bodyagin, H. Kresse, S. Diele, G. Pelzl, W. Weissflog. *Angew. Chem. int. Ed.*, **44**, 774 (2005).
[7] H.T. Nguyen, J.P. Bedel, J.C. Rouillon, J.P. Marcerou, M.F. Achard. *Pramana*, **61**, 395 (2003).
[8] W. Weissflog, H. Nadasi, U. Dunemann, G. Pelzl, S. Diele, A. Eremin, H. Kresse. *J. mater. Chem.*, **11**, 2748 (2001).
[9] H.N. Shreenivasa Murthy, B.K. Sadashiva. *Liq. Cryst.*, **29**, 1223 (2002).
[10] R. Amaranatha Reddy, B.K. Sadashiva. *Liq. Cryst.*, **30**, 273 (2003).
[11] B.K. Sadashiva, H.N.S. Murthy, S. Dhara. *Liq. Cryst.*, **28**, 483 (2001).
[12] S. Shubashree, B.K. Sadashiva, S. Dhara. *Liq. Cryst.*, **29**, 789 (2002).
[13] R. Achten, A. Koudijs, Z. Karzcmarzyk, A.T.M. Marcelis, E.J.R. Sudhölter. *Liq. Cryst.*, **31**, 215 (2004).
[14] H. Nadasi, W. Weissflog, A. Eremin, G. Pelzl, S. Diele, B. Das, S. Grande. *J. mater. Chem.*, **12**, 1316 (2002).
[15] R. Amaranatha Reddy, B.K. Sadashiva. *J. mater. Chem.*, **14**, 1936 (2004).
[16] R. Amaranatha Reddy, B.K. Sadashiva. *Liq. Cryst.*, **27**, 1613 (2000).
[17] J.P. Bedel, J.C. Rouillon, J.P. Marcerou, M. Laguerre, H.T. Nguyen, M.F. Achard. *J. mater. Chem.*, **12**, 2214 (2002).
[18] R. Amaranatha Reddy, B.K. Sadashiva. *J. mater. Chem.*, **12**, 2627 (2002).
[19] R. Amaranatha Reddy, B.K. Sadashiva. *Liq. Cryst.*, **30**, 1031 (2003).
[20] R. Amaranatha Reddy, V.A. Raghunathan, B.K. Sadashiva. *Chem. Mater.*, **17**, 274 (2005).
[21] R. Amaranatha Reddy, B.K. Sadashiva, V.A. Raghunathan. *Chem. Mater.*, **16**, 4050 (2004).
[22] H.N. Shreenivasa Murthy, B.K. Sadashiva. *Liq. Cryst.*, **31**, 1337 (2004).
[23] H.N. Shreenivasa Murthy, B.K. Sadashiva. *J. mater. Chem.*, **14**, 2813 (2004).
[24] H.N. Shreenivasa Murthy, B.K. Sadashiva. *Liq. Cryst.*, **31**, 1347 (2004).
[25] G. Dantlgraber, D. Shen, S. Diele, C. Tschierske. *Chem. Mater.*, **14**, 1149 (2002).
[26] J.P. Bedel, J.C. Rouillon, J.P. Marcerou, M. Laguerre, H.T. Nguyen, M.F. Achard. *Liq. Cryst.*, **27**, 1411 (2000).
[27] R. Achten, R. Cuypers, M. Giesbers, A. Koudijs, A.T.M. Marcelis, E.J.R. Sudhölter. *Liq. Cryst.*, **31**, 1167 (2004).
[28] G.S. Lee, Y.-J. Lee, S.Y. Choi, Y.S. Park, K.B. Yoon. *J. Am. chem. Soc.*, **122**, 12151 (2000).
[29] R. Achten, A. Koudijs, M. Giesbers, A.T.M. Marcelis, E.J.R. Sudhölter. *Liq. Cryst.*, **32**, 277 (2005).